Microstructure and mechanical characterization of NiCrBSi alloy and NiCrBSi-WC composite coatings produced by flame spraying

Rachida Rachidi[a,*], Bachir El Kihel[a], Fabienne Delaunois[b]

[a] Département de Génie industriel, Ecole Nationale des Sciences Appliquées, Université Mohamed Premier, Boite Postale 669, 60000 Oujda, Morocco
[b] Service de Métallurgie, Faculté Polytechnique, 56 Rue de l'Epargne, Université de Mons, 7000 Mons, Belgium

ABSTRACT

In this work, an experimental study is conducted on the microstructure and mechanical properties of NiCrBSi and NiCrBSi reinforced with WC coatings, produced onto mild steel substrate by flame spraying technique. The resulting layers were analyzed using optical microscopy, scanning electron microscopy (SEM) coupled with energy dispersive X-ray spectroscopy (EDX) and X-ray diffraction (XRD) analysis. Roughness measurements were made using a roughness measuring system. Microhardness tests were carried out using a microdurometer operating with Vickers indenter and the load being 3N. The results show that the microstructure contain some inhomogeneities such us pores, microcracks for the composite coating and oxides. The XRD analysis reveal that the phases present within the coatings are different from the initial powders. In addition, the presence of WC hard particles makes the hardness of the composite coating much higher than the metal alloy.

1. Introduction

Nowadays, NiCrBSi coatings are among the most widely used coatings in a variety industrial applications, to protect materials against wear, corrosion and oxidation at high temperature conditions up to 800 °C [1,2]. For example, they are applied to components such as gas turbines, roller, piston rods, wearing plates, tools, extruders, plungers, rolls for rolling mills, agricultural and mining machineries served in hostile condition [3,4], and in many studies, they are used as a replacements for harmful hard chromium coatings to the environment [5]. The presence of the chromium element is responsible for corrosion oxidation resistance, while boron and silicon is decreasing the alloy's melting point, which limits the rate of unmelted particles. The presence of carbon allows creating carbides responsible to increase coating hardness and wear resistance. The composition of self-fluxing NiCrBSi alloy also allows its fusion after the coating step by a laser or flame remelting process [6–8] to increase its functional properties, including the homogenization of the microstructure and decreasing the porosity level. NiCrBSi alloy took a great part in literature; many studies exist on their microstructural and tribological performance [9,10]. Moreover, metallic coatings such as NiCrBSi are a less expensive alternative to other materials, such as cermet powders, which are extremely expensive. Indeed, the properties of ceramic and cermet coatings are reduced at high temperature; while metal alloys retain good mechanical

properties in hot environments and are thus preferred for high temperature applications. However, because of environmental conditions that may be more critical in some applications, innovative materials known as metal matrix composites (MMC) are used. They provide in many cases, better wear resistance thanks to the combination of performances conferred by the metal matrix and those conferred by the reinforcing phase. The choice of appropriate reinforcing phase depends on the required properties. For example, the addition of WC ceramic particles is preferred to increase hardness and wear resistance at room temperature because of its exceptional mechanical properties [11–13]. However, other materials are used as reinforcement phase such as TiC, SiC, WC-Co, Cr_3C_2 and NbC, because of their high hardness and good wear resistance [14–18]. Note that the polishing operation is difficult in the case of coatings containing carbides particles. Generally, such coatings can be deposited by cladding laser and thermal spray technique.

Thermal spraying is a surface treatment method by coating, combining various techniques namely oxyacetylene flame spraying, HVOF spraying, electric arc spraying, atmospheric plasma spraying and cold spraying [19]. This process is used for repair of damage and worn out machine parts, and for the protection of new parts from wear and corrosion. The principle of thermal spray is to introduce the feedstock material in a heating zone (flame, plasma, arc) where it is melted, accelerated and then projected onto the surface to be coated where rapid

* Corresponding author.
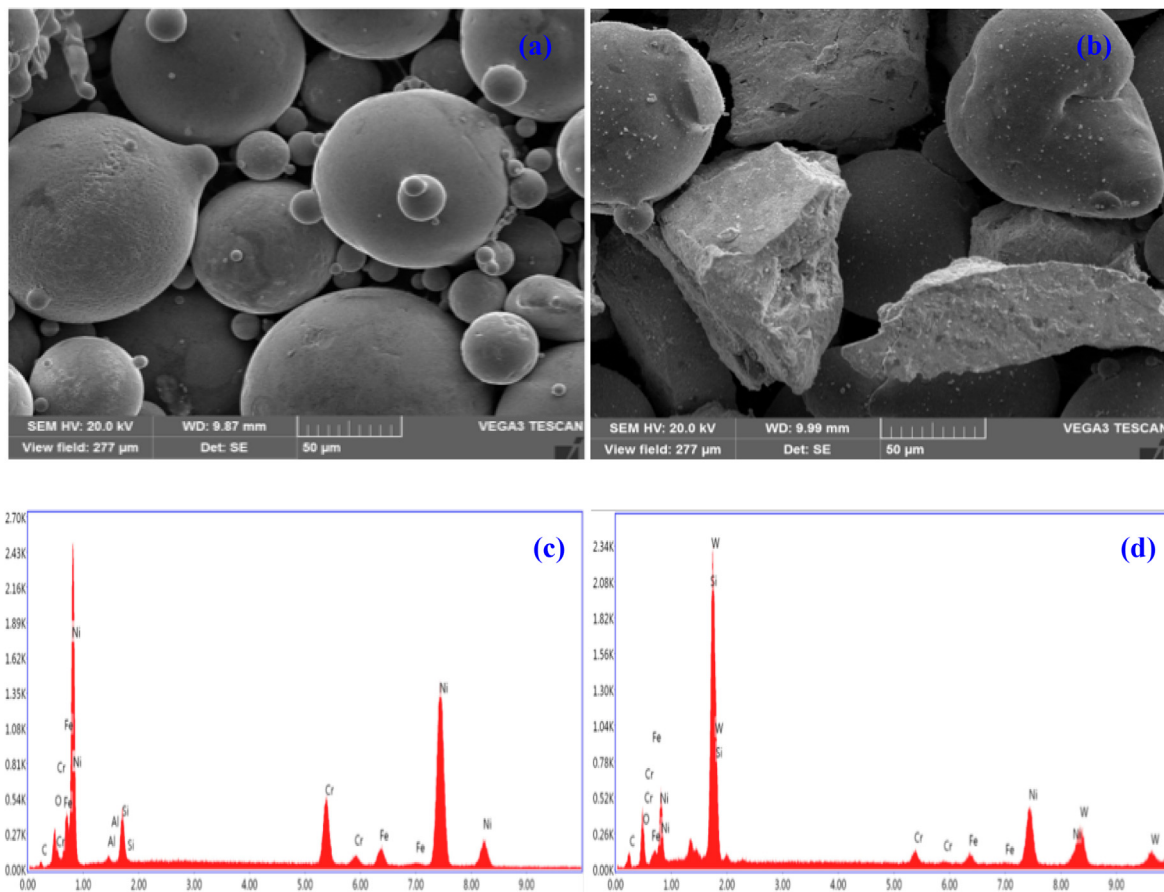 *E-mail address:* r.rachidi@ump.ac.ma (R. Rachidi).

Fig. 1. Morphology of (a) NiCrBSi powder, (b) NiCrBSi-WC powder, (c) EDX analysis of NiCrBSi powder and (d) EDX analysis of NiCrBSi-WC powder.

Table 1
Chemical composition of NiCrBSi and NiCrBSi-WC powders.

Composition (wt%)							
Powder	Ni	Cr	B	Si	Fe	C	WC
NiCrBSi	Balance	14.8	3.1	4.3	3.7	0.75	–
NiCrBSi-WC	Balance	7.3	3.3	4.5	6.3	0.25 max	60

Table 2
Coating deposition parameters.

Parameters	
Spray distance	20–30 mm
Spray angle	60° to 90°
Acetylene flow rate	60 SLPM
Oxygen flow rate	260 SLPM
Acetylene pressure	7 bar (700 KPa)
Oxygen pressure	10 bar (1 MPa)
Powder feed speed	Transported by gravity

Table 3
Roughness measurement.

Coating	Roughness Ra (µm)
NiCrBSi	11 ± 0.5
NiCrBSi-WC	6.45 ± 0.9

solidification and deposit build-up occurs [20]. Metals, ceramics, composites, and some polymeric materials in the form of powder, or wire can be deposited on materials generally ductile to improve their corrosion and wear resistance. For thermal spray process, deposits have generally a lamellar structure [6] if they are not post-treated and the main adhesion mechanism is mechanical resulting relatively low bond strength. The microstructure (presence of pores, oxides and/or un-melted particles) and hence the quality of the produced coating results directly from the used deposition technique [19]. The flame spray technique has some disadvantages compared with the HVOF or plasma spray techniques. It produced coating with modest quality including pores, oxides, cracks and relatively poor adhesion to the substrate [6], but it also has certain advantages such as its being more economical, easier to implement and more adaptable to a wide range of materials. It provides a good wear and corrosion resistance, especially after thermal treatment [21]. That made it one of the most used techniques for the manufacture of tribological coatings to a wide variety of applications, including dry wear resistance or in the presence of lubricants, wear resistance at high temperature, tribocorrosion conditions, restoration of worn components. Oxyacetylene torches are using acetylene as the fuel and oxygen to generate high combustion temperatures up to 2600 °C. The particle velocities are typically in the range of 150–300 m/s de-pending on the alloy density, particle shape and surface texture.

This work is focused on the morphology, the microstructure evolution of two coatings: NiCrBSi alloy and NiCrBSi alloy reinforced with 60% by weight of WC, deposited onto S235JR mild steel substrates beforehand prepared using oxyacetylene flame spraying process. Our contribution will have an interesting economic impact aiming at im-proving the wear resistance of mechanical parts damaged in service. The microstructure and chemical composition of the manufactured layers were characterized using optical microscopy (OM), scanning electron microscopy (SEM) coupled with energy dispersive X-ray spectroscopy (EDX) and X-ray diffraction (XRD). The roughness mea-surements of as-sprayed coatings were carried out using a roughness
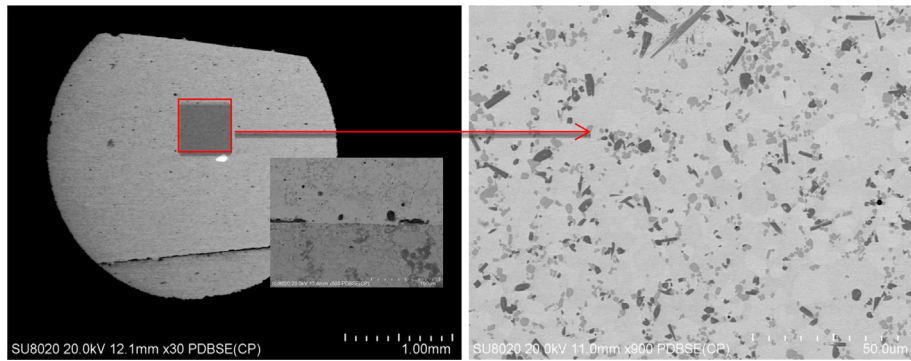
Fig. 2. Microstructure of NiCrBSi coating deposited by flame thermal spraying technique.
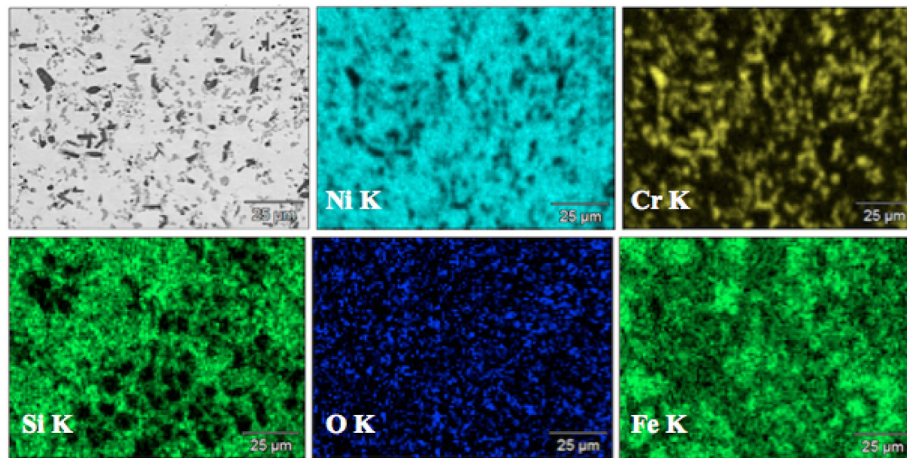

Fig. 3. Elemental EDX mapping of NiCrBSi coating.

measuring system. This work was extended to study the microstructure effect on the microhardness of coatings. The wear performance of theses coatings under two different wear modes is also studied and presented in another scientific paper [22].

2. Experimental procedure

2.1. Materials and deposition technique

Two commercially powders used as feedstock material were identified from Castolin Eutectic Company (Fig. 1). Ni-based alloy powder, designated Borotec 10009, has particle size 53–150 μm, good castability because of their spherical morphology and hardness of 58 HRC. The second powder designated Eutalloy 10112 consisting of a mixture of NiCrBSi alloy with 60 wt% of WC. Its particle size is 20–150 μm (typical of thermal spraying), a non-spherical angular morphology and hardness of 63 HRC. The melting temperature of the NiCrBSi-WC powder was 1000 °C. The chemical compositions of the two powders are given in Table 1 (provider data). S235JR mild steel was used as substrate with tensile strength of 235 MPa and the nominal chemical composition (wt %) is: C 0.17% max., S 0.045% max., Mn 1.40% max., P 0.045% max., N 0.009% max. and Fe balance. The substrate selection was guided by the common use of this steel in industry, due to its very low cost and also by the small difference of the linear thermal expansion coefficients between the steel and the NiCrBSi alloy; mild steel has a coefficient equal to $11 \times 10^{-6} \, \text{K}^{-1}$ against $13.6 \times 10^{-6} \, \text{K}^{-1}$ for the NiCrBSi alloy) which limits the delamination risk at the interface between substrate and the coating layer by thermal effect. According to literature, the mild steel is used as substrate for the manufacturing of flame thermal spray coatings. The preliminary implementation of thermal or mechanical treatment is not necessary for this type of steel.

Prior to the coating process, the specimens are manufactured from S235JR mild steel bars that were cut and then machined into discs with 50 mm in diameter and 10 mm in thickness and also rectangular specimens with the dimensions 60 mm × 50 mm × 10 mm. Then, two specimen surfaces were cleaned by means of a shot-blasting gun, using alumina particles (Al_2O_3) with 425–600 μm sizes and the pressure was 6 bar (0,6 MPa). The gun-to-substrate distance is maintained at 120 mm and the blasting angle at 45°. The purpose of this step is to remove the oxides present on the surface and to create a roughness profile for good adhesion coating on the substrate. The blasting operation under the mentioned conditions did not seem the right choice. Another method has been proposed, namely rectification. The specimens were rectified to create roughness profile to the surface (about 7 μm) and were coated in local company of mechanical production. The deposition was performed using oxyacetylene flame thermal spraying technique with SuperJet Eutalloy (SuperJet Eutalloy, Castolin Eutectic) torch. The treatment parameters used in this study are summarized in Table 2 below.

A set of specimens was coated with NiCrBSi powder alloy and another set with NiCrBSi-WC powder. The thickness of the obtained coatings was measured by means of optical microscopy and scanning electron microscopy and the average thickness is about 2 mm. The substrate surface preparation is influenced by two parameters: the creation of a roughness profile on the surface to increase adhesion force and the preheating of the substrate to reduce thermal stresses. The surface roughness of as-sprayed coatings was measured using TR200 TIME roughness tester. The parameter used to characterize surface roughness is the arithmetic average Ra on a measuring length L of 12.5 mm, with 5 measurements taken on each surface (Table 3). The substrate preheating was carried out with oxyacetylene flame for 5 min each specimen. During the flame spraying, the substrate temperature
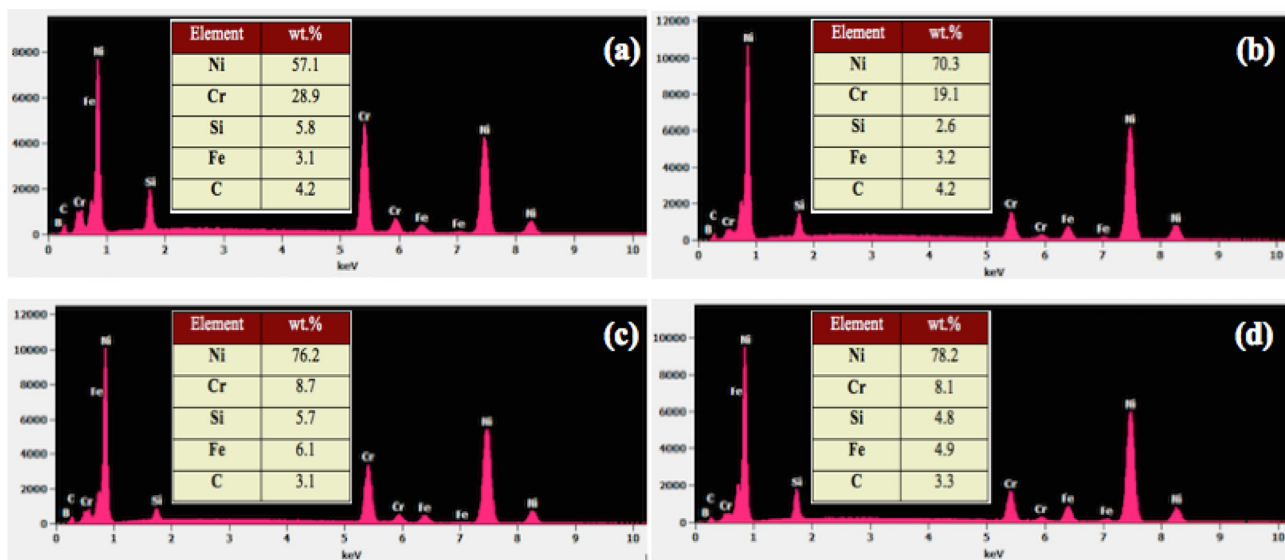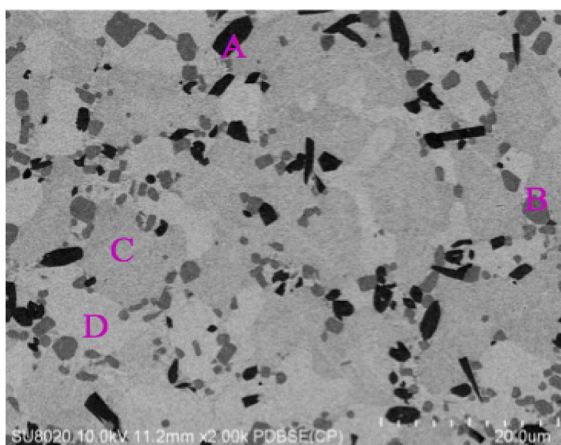
Fig. 4. SEM micrograph and elemental EDX analysis (wt%) at spots: (a) spot A, (b) spot B, (c) spot C and (d) spot D for NiCrBSi coating.
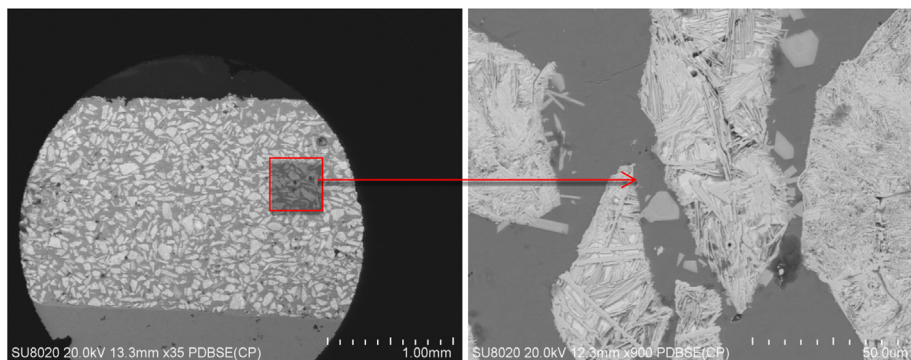

Fig. 5. Microstructure of NiCrBSi-WC coating deposited by flame thermal spraying technique.

increases from the initial preheat temperature.

2.2. Microstructural analysis

After the coating process, the coated specimens and other basic steel are cut, hot mounted with resin to allow easier handling of the specimens and ensure the flatness of the surface during polishing. Then, they were ground with SiC abrasive paper and finally polished with diamond suspension to obtain a specular surface condition, using automatic polisher from STRUERS to ensure good reproducibility. Thereafter, the specimens were placed in an ultrasonic bath and cleaned with demineralized water and dried with compressed air. Finally, they were chemically etched using Murakami etchant for composite coatings and Nital etchant for both substrate and Ni-based coatings, making the microstructure observation easier. These specimens were characterized (both on surface and cross-section) by 3D optical microscope (KH-8700, Hirox) and scanning electron microscope SEM (SUB020, Hitachi). By means of SEM, the basic elements of studied layers namely Ni, Cr, Si, C,
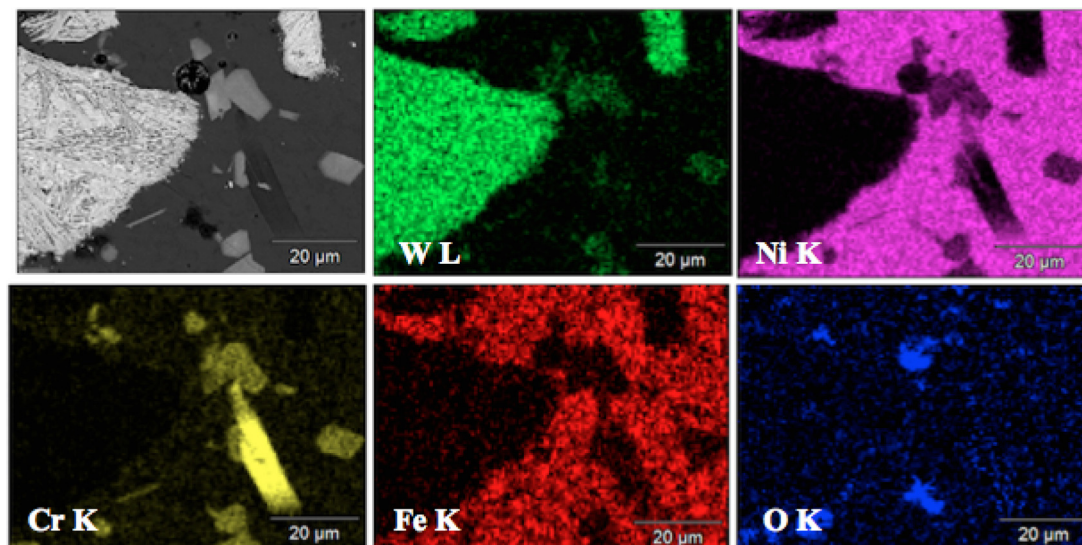
Fig. 6. Elemental EDX mapping of reinforced NiCrBSi-WC coating.

W and Fe were detected. However, due to the detection sensitivity limit, the weight percentage of boron element B cannot be determined, although its presence can be confirmed. The chemical composition of coatings was analyzed by Energy-Dispersive X-ray spectroscopy (EDX). A detailed analysis of phases and their composition was made by X-ray diffraction technique (XRD) using a diffractometer (D5000, Siemens). The voltage and the current were 40 kV and 100 mA respectively. The diffraction angle 2θ was between 20° and 80°.

2.3. Microhardness

The microhardness measurements are made by means of Vickers microhardness tester (M-400-A, LECO) under 300 gf load, on metallographic sections, perpendicular to the deposit surface and also on cross-sections, knowing that the hardness varies depending on the sections directions owing to the characteristic anisotropy of thermal spray coatings microstructure. The residence time is 7 μm in the case of steel, 5–6 μm for NiCrBSi coating and about 4 μm for NiCrBSi-WC composite coating. An average hardness was calculated from 20 indentations for each specimen and the calculation formula (1) is as follows:

$$HV = \frac{2F \times \sin(136°/2)}{g \times d^2} = 0,189 \times F/d^2 \tag{1}$$

where HV is the Vickers hardness, F is the applied force (N), d is the diagonals indentation average (mm) and g is the gravity (m/s^{-2}) 9,80665.

3. Results and discussion

3.1. Microstructural characterization of coatings

3.1.1. NiCrBSi coating

Fig. 2 exhibits the SEM microstructure of NiCrBSi coating. Regarding the microstructure, it is clear that coating does not clearly reveal the lamellar structure as reported in literature relative to thermal spray coatings [23–26]. This result shows that NiCrBSi alloy is completely melted during the spraying process under the used parameters. The similar microstructure is presented by [27]. As global view of coating cross-section, it can be also observed the presence of certain level of pores but not too pronounced. However, no cracking was observed. According to literature [28], the impact temperature and the velocity of particles, among other parameters, governing the spreading degree of the splats forming the deposit. The low particle velocity

characteristic of flame thermal spraying process ensures that some particles are not well spread at the time of impact on the substrate and therefore, this phenomenon promotes the presence of pores in coating. The interface profile appears to be detached from the substrate, but in reality it is just a defect owing to the cutting method where SiC disc was used at the beginning, which is not suitable for this type of coatings.

Fig. 3 shows an elemental analysis of the NiCrBSi coating. Looking at the microstructure of the NiCrBSi coating, it contains several differently coloured and dispersed phases. The small particles dispersed within the Ni solid solution matrix should be borides and carbides formed during deposition. From the elemental analysis, we can notice the presence of small quantities of oxides and this may be owing to the relatively long residence time of sprayed particles in the flame. Indeed, the particles are heated to a high temperature degree and the chemical reaction with oxygen present in the environment is enhanced. Additionally, the low velocity of the particles and the relatively long flight time increases the particles temperature. This can be considered as an explanation for the presence of oxides in the coating layer.

The chemical composition is illustrated in Fig. 4. It can be noticed that the distribution of different phases within the coating has good overall homogeneity. To identify each phase, the EDX analysis was performed. The measurement spots (A, B, C and D) are shown and the measurement results are summarized in Fig. 4. The darker phase A present the maximum amount of Chromium (28.9% Cr) followed by phase B (19.1% Cr) with an increase in Ni amount. According to literature, phase A correspond to CrB and phase B correspond to Cr_7C_3. Phase C (76.2% Ni) and phase D (78.2% Ni) contain the maximum of Ni and correspond to Ni/Ni_3B and Ni solid solution respectively.

3.1.2. NiCrBSi-WC coating

Fig. 5 shows SEM micrograph of the general appearance of the NiCrBSi-WC cross-section. The thermal sprayed composites are composed of a Ni solid solution matrix (dark gray) and a second phase known as reinforcement, which is WC in our study. The WC particles are easily identifiable by their different (light grey) color and angular shape; WC particles have kept the same shape as in initial powder. During the coating process, the feedstock material begins to melt when the temperature reached its melting point, which means that the melting point of NiCrBSi is reached, but the WC particles are not completely melted. As we can see, the layer structure is modified by adding WC particles but remains homogeneous; WC particles are well distributed in the Ni solid solution matrix. The matrix plays, in most cases, a role in distributing stresses homogeneously in the coating. The
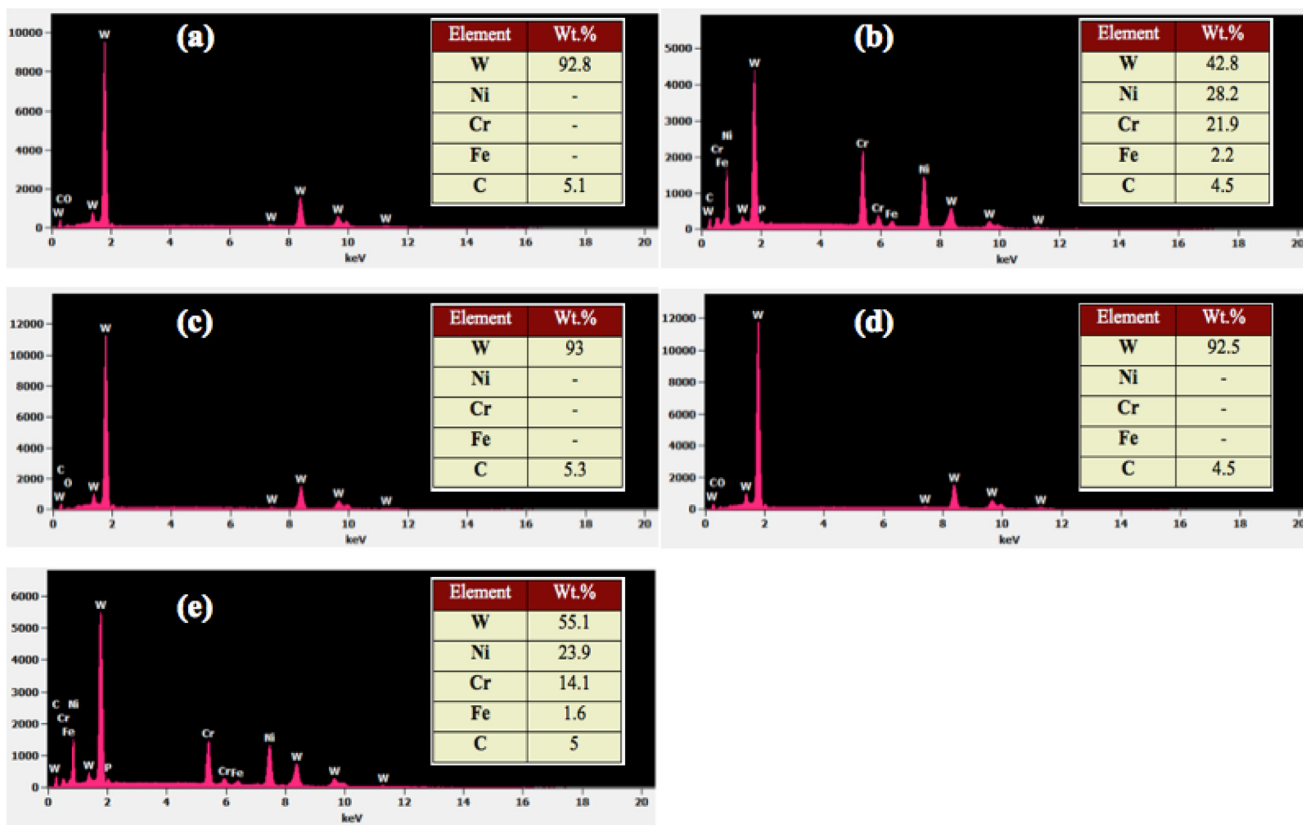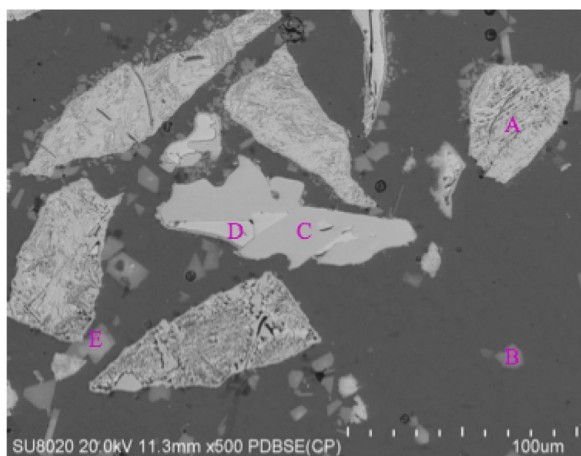
Fig. 7. SEM micrograph and elemental EDX analysis (wt%) at spots: (a) spot A, (b) spot B, (c) spot C, (d) spot D and (e) spot E for NiCrBSi-WC coating.
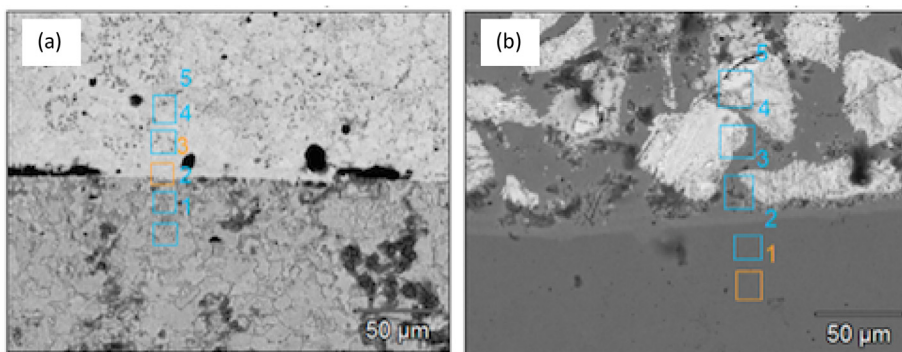

Fig. 8. SEM micrograph of (a) substrate/NiCrBSi and (b) substrate/NiCrBSi-WC coatings interface.

Table 4
The EDX analysis of the component diffusion on substrate/NiCrBSi coating interface.

Composition (wt%)				
Area	Ni	Cr	Si	Fe
1	–	–	–	96.4
2	–	0.3	–	91.9
3	0.7	0.4	0.3	92.4
4	68.9	4.2	4.7	15.8
5	81.7	8.4	3.6	4.3

Table 5
The EDX analysis of the component diffusion on substrate/NiCrBSi-WC coating interface.

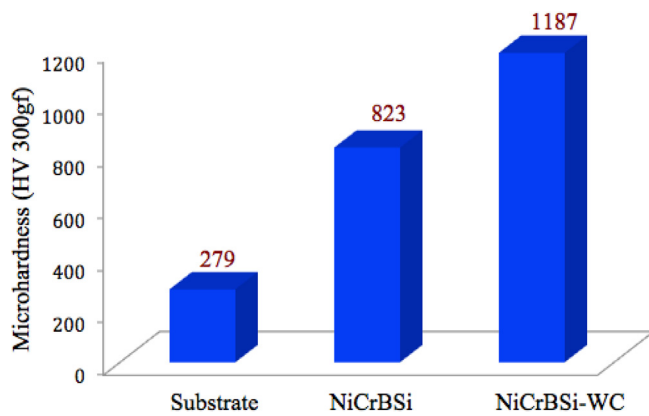| Composition (wt%)					
Area	W	Ni	Cr	Si	Fe
1	–	–	0.2	0.3	96.4
2	–	–	–	–	97.6
3	28.6	19.7	1.6	–	39.2
4	63.3	14.4	1.4	–	13.5
5	74	5.2	1.2	–	3.4

Fig. 9. Microhardness results measured on steel substrate, NiCrBSi and NiCrBSi-WC coating surface.
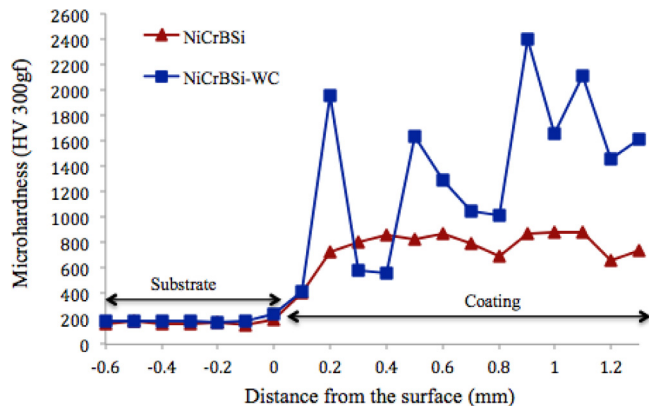

Fig. 10. Microhardness variation along the depth of steel substrate, NiCrBSi and NiCrBSi-WC coatings.

reinforced NiCrBSi coating has a similar level of pores to that of the NiCrBSi coating with presence of microcracks in the matrix and tungsten carbide particles. These defects are typical of coatings produced by thermal spraying. In the case of WC reinforced coatings, the cracking

level could not be completely avoided but can be minimized by reducing the WC content [7].

The same characterization procedure relative to NiCrBSi coating is applied in the case of reinforced NiCrBSi coating. In Fig. 6 is shown a mapping of the various elements present in the layer.

The presence of oxide content is also noticed in the case of reinforced NiCrBSi coating. The elemental analysis of the reinforced NiCrBSi coating was performed by EDX in order to identify each phase. The measurement spots (A, B, C, D and E) and the measurement results are shown in Fig. 7. The phases A, C and D are mainly composed with WC, which correspond to 92.8% W, 93% W and 92.5% W respectively. These three phases seems to be one and the same phase, which is WC. During the spraying process, the surface of WC particles can be decomposed to form a brittle phase W_2C particle due to the overheating temperature (at 2600 °C) and the presence of oxygen. W_2C is more brittle than WC and WC has better wettability by molten metals and wear-resistance than W_2C does. Phases B and E can be WC and other carbides.

3.1.3. Substrate/coating interface analysis

Fig. 8 shows SEM micrographs of the substrate/NiCrBSi coating interface and the substrate/NiCrBSi-WC coating interface. The analysis of material diffusion on the interface by means of EDX technique is given in Tables 4 and 5.

The as-sprayed coatings produced by thermal spraying are principally adherent to the substrate by mechanical mechanism. This bond becomes metallurgical when a fusing treatment is applicable. According to Fig. 8, the adhesion between substrate and NiCrBSi coating seems to be good with presence of low pores in the interface. The interface substrate/composite coating is practically pore-free and the adhesion is much higher than in the case of NiCrBSi coating. It is important to note that no fusing treatment is used in this study. The EDX analysis of the interface for both coatings (Tables 4 and 5) shows that dilution of the substrate has occurred, making the adhesion better. The similar findings are reported in literature [29].

3.2. XRD phase analysis

The Ni-based matrix contains Nickel, Chromium, Iron, Silicon and Boron. The binary phase diagrams such as NiCr, NiB, and NiSi provide information on the effects of individual alloying elements on the melting temperature of the NiCrBSi alloy [30]. They show that the presence of Cr, Si and B elements reduce the melting temperature point of nickel to 1040 °C, which is relatively low melting temperature for the NiCrBSi alloy. At temperature 1110 °C, the entire coating becomes liquid [6]. Furthermore, these three elements play a role in forming hard borides and carbides, owing to improve the mechanical properties of the produced coating. The NiCrBSi is made of a Ni-rich solid solution phase γ-Ni and low content of Ni-Ni_3B eutectic [7]. When the sprayed alloy solidified from high temperature, several possible borides, carbides and silicates may be created, such as, Ni_2B, CrB, Ni_5Si_3, $Ni_{13}Si_{12}$, Ni_3Si, $(Cr,Fe)_7C_3$ and $Cr_{23}C_6$. Which one is produced depends to a large extent on the composition of the alloy and the solidification process. Kim et al. [7] reported that, during remelting treatment, the chromium carbide precipitate (Cr_7C_3) could be increase where the carbon content in the chemical composition of a coating exceeds 0.8 wt%. In addition, if the content of boron in the coating exceeds 2 wt%, the microstructure contains chromium boride (CrB) precipitates. It was reported the formation of γ-Ni and Ni-Ni_3B [6], CrB and $(Cr,Fe)_7C_3$ [10,29]. Based on the XRD analysis, the NiCrBSi coating was mainly composed by γ-Ni, CrB, Ni_3B phases. With regard to the XRD results and the microstructure of the NiCrBSi coating, the dark gray phase is chromium boride CrB, while the light phases can be identified as the γ-Ni solution and Ni_3B. However, the presence of Cr_7C_3 has not been confirmed by this analysis. The XRD analysis of the composite coating confirms the presence of WC, γ-Ni solid solution and a small amount of Ni_3B phase in the

coating. Other precipitates such as W_2C and Cr_7C_3 were found in the composite coating matrix add to γ-Ni solution and Ni_3B. These phase compositions are in accord with EDX analysis and other works reported in literature [27].

3.3. Coatings hardness

The addition of hard particles to the metal alloy can increase the hardness of the coating. The microhardness tests were performed onto mild steel substrate and coating layers (both on surface and cross-section). The measurements were carried out in Vickers microhardness under 300 gf load. The results are shown in Figs. 9 and 10.

3.3.1. Surface measurements

The average microhardness of the NiCrBSi coating ($823\,HV_{0.3}$) is much higher than those reported in the literature in the range of 700–750 HV [27,7,31]. The reason may be the cohesion of coating as well as the formation of small precipitates like chromium borides and carbides (according to their quantity and size), which are distributed in the microstructure [1]. From the comparison of the results, it is interesting to see that the NiCrBSi-WC layers are the hardest on the surface ($1187\,HV_{0.3}$). Indeed, the presence of WC hard ceramic particles within the coating lead to an increase in the microhardness value.

3.3.2. Cross-section measurements

Fig. 10 shows the microhardness measurements on the cross-section for the coatings. It is clear that in the presence of the NiCrBSi and the NiCrBSi-WC coatings, the hardness is significantly higher compared to the steel substrate. From the interface steel/coating, the NiCrBSi coating has a uniform hardness in the range of 800 HV with uniform behavior. The NiCrBSi-WC coating shows a significantly higher hardness, but with significant variations from one point to another, which can be attributed to the WC particles, which are agglomerate in the matrix. It is interesting to see that the microhardness decreases near the interface because of the diffusion of the Fe from the substrate. The micro-cracks in the NiCrBSi-WC coating can be justified by its high hardness and low fracture toughness.

4. Conclusions

The microscopic morphology, chemical composition, phases and distribution of WC particles in the flame sprayed NiCrBSi and NiCrBSi-WC coatings onto mild steel were investigated by means of SEM and X-ray diffraction techniques. The results of this study are as bellow:

- The lamellar microstructure, which is characteristic of thermal sprayed coatings, has not been revealed for both NiCrBSi and NiCrBSi-WC coatings.
- The produced coatings have a low level of porosity. The micro-cracks have appeared in the metal matrix and also in the WC hard ceramic particles in the case of the composite coating.
- The EDX analysis shows that diffusion is produced at the substrate/coating interface. In this case, the adhesion mechanism becomes metallurgical.
- The NiCrBSi matrix contains γ-Ni, Ni_3B and CrB phases. The presence of Boron element in the Ni-based alloy beside of Silicon element is responsible for reducing the melting point of the alloy. Furthermore, it plays a role in forming hard borides, which improves the mechanical properties of the coating.
- The WC hard ceramic particles in the composite coating are responsible for forming W_2C and carbides Cr_7C_3 distributed in the metallic matrix.
- The microhardness tests carried out on coatings both on the surface and the cross-sections demonstrate that the presence of WC hard ceramic particles in coating increases its hardness.

The processing parameters namely the spray distance, the spray angle, oxygen/acetylene ratio, the substrate surface condition are very important and should be optimized to get the high-quality coating, which was free of pores and cracks and good adhesion to the substrate. The increase in hardness has an effect on the wear resistance of the coatings. Therefore, supplementary works concerning performance characterization of these coatings in terms of wear resistance were performed.

References

[1] P.R. Reinaldo, A.S.C.M.D. Oliveira, NiCrSiB coatings deposited by plasma transferred Arc on different steel substrates, J. Mater. Eng. Perform. 22 (2013) 590–597.

[2] T.S. Sidhu, S. Prakash, R.D. Agrawal, Hot corrosion behaviour of HVOF-sprayed NiCrBSi coatings on Ni and Fe-based superalloys in Na2SO4-60% V2O5 environment at 900 °C, Acta Mater. 54 (2006) 773–784.

[3] S.P. Lu, O.H. Kwon, Y. Guo, Wear behavior of brazed WC/NiCrBSi(Co) composite coatings, Wear 254 (2003) 421–428.

[4] C. Guo, J. Chen, J. Zhou, J. Zhao, L. Wang, Y. Yu, H. Zhou, Effects of WC–Ni content on microstructure and wear resistance of laser cladding Ni-based alloys coating, Surf. Coat. Technol. 206 (2012) 2064–2071.

[5] S. Houdkova, F. Zahalka, M. Kasparova, L.M. Berger, Comparative study of thermally sprayed coatings under different types of wear conditions for hard chromium replacement, Tribol. Lett. 43 (2011) 139–154.

[6] Z. Bergant, J. Grum, Quality improvement of flame sprayed, heat treated, and remelted NiCrBSi coatings, J. Therm. Spray Technol. 18 (2009) 380–391.

[7] H.J. Kim, S.Y. Hwang, C.H. Lee, J. Philippe, Assessment of wear performance of flame sprayed and fused Ni-based coatings, Tribol. Lett. 172 (2003) 262–269.

[8] R. González, M. Cadenas, R. Fernández, J.L. Cortizo, E. Rodríguez, Wear behaviour of flame sprayed NiCrBSi coating remelted by flame or by laser, Wear 262 (2007) 301–307.

[9] A. Arcondeguy, A. Grimaud, A. Denoirjean, G. Gasgnier, C. Huguest, B. Pateyron, G. Montavon, Flame-sprayed glaze coatings: effects of operating parameters and feedstock characteristics onto coating structures, J. Therm. Spray Technol. 16 (2007) 978–990.

[10] C. Navas, R. Colaço, J. Damborenea, R. Vitar, Abrasive wear behaviour of laser clad and flame sprayed-melted NiCrBSi coatings, Surf. Coat. Technol. 200 (2006) 6854–6862.

[11] A. Martin, J. Rodriguez, J.E. Fernández, R. Vijande, Sliding wear behaviour of plasma sprayed WC-NiCrBSi coatings at different temperatures, Wear 251 (2001) 1017–1022.

[12] C.P. Paul, S.K. Moshra, P. Tiwari, L.M. Kukreja, Solid-particle erosion behaviour of WC/Ni composite clad layers with different contents of WC particles, Opt. Laser Technol. 50 (2013) 155–162.

[13] J. Przybylowicz, J. Kusinski, Structure of laser cladded tungsten carbide composite coatings, J. Mater. Process. Technol. 109 (2001) 154–160.

[14] A. Maatta, U. Kanerva, P. Vuoristo, Structure and tribological characteristics of HVOF coatings sprayed from powder blends of Cr3C2-25NiCr and NiCrBSi alloy, J. Therm. Spray Technol. 20 (2011) 366–371.

[15] H. Chen, C. Xu, J. Qu, I.M. Hutchings, P.H. Shipway, J. Liu, Sliding wear behaviour of laser clad coatings based upon a nickel-based self-fluxing alloy co-deposited with conventional and nanostructured tungsten carbide–cobalt hardmetals, Wear 259 (2005) 801–806.

[16] D. Gang, Y. Biao, D. Qilin, Y. Ting, Microstructure and wear resistance of in situ NbC particles reinforced Ni-based alloy composite coating by laser cladding, J. Wuhan Univ. Technol. -Mater. Sci. 27 (2012) 231–237.

[17] X. Wang, M. Zhang, Z. Zou, S. Qu, Microstructure and properties of laser clad TiC + NiCrBSi + rare earth composite coatings, Surf. Coat. Technol. 161 (2002) 195–199.

[18] S. Buytoz, M. Ulutan, S. Islak, B. Kurt, O.N. Çelik, Microstructural and wear characteristics of high velocity oxygen fuel (HVOF) sprayed NiCrBSi–SiC composite coating on SAE 1030 steel, Arab J. Sci. Eng. 38 (2013) 1481–1491.

[19] S.V. Joshi, M.P. Srivastava, Plasma spraying of WC-Co Part II: experimental study of particle deposition and coating microstructure, J. Therm. Spray Technol. 2 (1993) 133–136.

[20] J. Tikkanen, K.A. Gross, C.C. Berndt, V. Pitkänen, J. Keskinen, S. Raghu, M. Rajala, J. Karthikeyan, Characteristics of the liquid flame spray process, Surf. Coat. Technol. 90 (1997) 210–216.

[21] G.J. Li, J. Li, X. Luo, Effects of post-heat treatment on microstructure and properties

of laser cladded composite coatings on titanium alloy substrate, Opt. Laser Technol. 65 (2015) 66–75.

[22] R. Rachidi, B. Elkihel, F. Delaunois, V. Vitry, D. Deschuyteneer, Wear performance of thermally sprayed NiCrBSi and NiCrBSi-WC coatings under two different wear modes, J. Mater Environ. Sci. 8 (2017) 4550–4559.

[23] J. Voyer, Wear-resistant amorphous iron-based flame-sprayed coatings, J. Therm. Spray Technol. 19 (2010) 1013–1023.

[24] N.L. Parthasarathi, D. Muthukannan, B. Utpal, Effect of plasma spraying parameter on wear resistance of NiCrBSiCFe plasma coatings on austenitic stainless steel at elevated temperatures at various loads, Mater. Des. 36 (2012) 141–151.

[25] E. Sadeghimeresht, N. Markocsan, P. Nylén, Comparative study on Ni-based coatings prepared by HVAF, HVOF and APS methods for corrosion protection applications, J. Therm. Spray Technol. 25 (2016) 1604–1616.

[26] L. Liming, X. Haifeng, X. Jinkun, W. Xinlong, G. Zhang, C. Zhang, Effect of heat treatment on structure and property evolutions of atmospheric plasma sprayed NiCrBSi coatings, J. Surface Coat. Technol. 325 (2017) 548–554.

[27] Z.Q. Zhang, H.D. Wang, B.S. Xu, G.S. Zhang, Characterization of microstructure and rolling contact fatigue performance of NiCrBSi/WC-Ni composite coatings prepared by plasma spraying, Surf. Coat. Technol. 261 (2015) 60–68.

[28] J. Mostaghimi, M. Pasandideh-Fard, S. Chandra, Dynamics of splat formation in plasma spray coating process, Plasma Chem. Plasma Process. 22 (2002) 59–84.

[29] T. Gomez-del Rio, M.A. Garrido, J.E. Fernandez, M. Cadenas, J. Rodriguez, Influence of the deposition techniques on the mechanical properties and microstructure of NiCrBSi coatings, J. Mater. Process. Technol. 204 (2008) 304–312.

[30] Alloy Phase Diagrams, ASM Handbook, ASM International, 2003 432, 692, and 1233.

[31] S. Huang, D. Sun, D. Xu, W. Wang, H. Xu, Microstructures and properties of NiCrBSi/WC biomimetic coatings prepared by plasma spray welding, J. Bionic Eng. 12 (2015) 592–603.